Structure of the bacterial flagellar hook and implication for the molecular universal joint mechanism

Fadel A. Samatey[1,2,3], Hideyuki Matsunami[1,2,3], Katsumi Imada[1,2,3], Shigehiro Nagashima[1,3], Tanvir R. Shaikh[4]*, Dennis R. Thomas[4], James Z. Chen[4], David J. DeRosier[4], Akio Kitao[5] & Keiichi Namba[1,2,3]

[1]*Dynamic NanoMachine Project, ICORP, JST, 1-3 Yamadaoka, Suita, Osaka 565-0871, Japan*
[2]*Graduate School of Frontier Biosciences, Osaka University, 1-3 Yamadaoka, Suita, Osaka 565-0871, Japan*
[3]*Protonic NanoMachine Project, ERATO, JST, 3-4 Hikaridai, Seika, Kyoto 619-0237, Japan*
[4]*W. M. Keck Institute of Cellular Visualization, Rosenstiel Basic Medical Sciences Research Center and Department of Biology, Brandeis University, Waltham, Massachusetts 02454-9110, USA*
[5]*Institute of Molecular and Cellular Biosciences, University of Tokyo, 1-1-1 Yayoi, Bunkyo, Tokyo 113-0032, Japan*

* Present address: Wadsworth Center, P.O. Box 509, Albany, New York 12201, USA

The bacterial flagellum is a motile organelle, and the flagellar hook is a short, highly curved tubular structure that connects the flagellar motor to the long filament acting as a helical propeller. The hook is made of about 120 copies of a single protein, FlgE, and its function as a nano-sized universal joint is essential for dynamic and efficient bacterial motility and taxis. It transmits the motor torque to the helical propeller over a wide range of its orientation for swimming and tumbling. Here we report a partial atomic model of the hook obtained by X-ray crystallography of FlgE31, a major proteolytic fragment of FlgE lacking unfolded terminal regions, and by electron cryomicroscopy and three-dimensional helical image reconstruction of the hook. The model reveals the intricate molecular interactions and a plausible switching mechanism for the hook to be flexible in bending but rigid against twisting for its universal joint function.

To propel themselves in their living environments towards favourable conditions and away from unfavourable ones, bacteria have developed highly sophisticated machinery called the flagellum. It is a complex molecular machine made of about 25 different proteins, each in multiple copies from a few to a few tens of thousands[1–3]. The flagellum can be divided into three parts: the basal body, the hook and the filament[4,5]. The basal body is a rotary motor[6,7], and its complex structure, which is made of about 20 proteins, begins inside the cell, spans the cell envelope including the cytoplasmic membrane, and extends well outside the cell[1,8]. The filament, a long tubular structure, is a helical assembly of some tens of thousands of copies of a single protein FliC (flagellin). Its polymorphic supercoiled forms permit it to function as a helical propeller, which switches its helical pitch and handedness depending on the swimming mode[9,10]. The hook, a short, highly curved tube, is a helical assembly of about 120 copies of a single protein, FlgE (refs 4, 5, 11, 12), also called the hook protein. The hook connects the basal body to the filament. Its flexibility permits it to transmit torque from the motor to the helical propeller when the two are not coaxial[6]. The hook allows the synchronous rotation of several filaments driven by their motors in a bundle formed behind the cell (swimming) as well as the uncoordinated rotation of individual, unbundled filaments in different orientations[6,9,10] (tumbling). An appropriate length and bending flexibility of the hook seem to be important for its universal joint function[13]. There are also two proteins, hook-associated protein 1 (HAP1) and 3 (HAP3), forming a very short hook-filament junction, which probably acts as a structural adaptor for a smooth transition between the two mechanically distinct structures: the hook is relatively flexible in bending, whereas the filament is much more rigid for its propeller function.

The hook of *Salmonella* flagella and its component protein FlgE have been studied by electron microscopy as well as by biochemical and physicochemical methods. The length of the hook is relatively well regulated to be 55 ± 6 nm (ref. 14), but it becomes much longer if there is a mutation in FliK or FlhB, two proteins involved in protein export and flagellar assembly. The helical packing of subunits in this abnormally long hook, called a polyhook, is the same as that in the normal hook[15]. This helical packing is distorted into a superhelical form, although with an amplitude and pitch smaller than those of the superhelical flagellar filament. The wild-type hook is thus a short segment of this superhelical form rather than a simply bent rod structure. The polyhook also shows polymorphism, transforming into distinct helical forms as well as a straight form depending on the solution condition such as pH, ionic strength and temperature[12,16–18]. The structures of various straight polyhooks studied by electron microscopy and helical image analysis have shown that the basic architecture of the hook is similar to that of the flagellar filament, which can be described as a tubular fibre made of 11 protofilaments or a helical symmetry of about 11 subunits per two turns of the 1-start helix[11,19], in spite of the fact that the hook protein and flagellin have very different amino acid sequences[20].

To understand the mechanism of this molecular universal joint, we have solved the structure of a core fragment of FlgE by X-ray crystallography at 1.8 Å resolution and built an atomic model of the hook by docking it into a density map of the hook obtained by electron cryomicroscopy and image analysis. The hook model now shows its complex molecular interactions and a possible switching mechanism to form a highly curved and twisted tubular structure within which individual protofilaments go through rather large and dynamic conformational changes for their rather extensive elongation and shortening as the curved hook rotates rapidly.

Structure of FlgE31

Because full-length FlgE, like FliC (flagellin), forms filaments not crystals, we cloned, overexpressed in *Escherichia coli* and crystallized a fragment named FlgE31, corresponding to residues 71–369 out of 402 and having a molecular mass of 31 kDa. This same trick works

©2004 Nature Publishing Group

for FliC (refs 21, 22). This fragment, which lacks both terminal regions that are unfolded in the monomeric form in solution[23], has two compact domains as judged from its calorimetric melting profile[24]. Indeed, the Cα backbone trace of FlgE31 revealed by X-ray crystallography actually shows two domains, D1 and D2, connected by a short stretch of two-strand anti-parallel β-sheet (Fig. 1). The orientation of FlgE31 in Fig. 1 (namely D1 at the bottom and D2 at the top) is that found in a hook whose cell proximal side is down; this orientation will be used throughout the paper.

In the atomic model, the amino-terminal segment from Gly 71 to Ala 144 and the carboxy-terminal segment from Pro 285 to Ser 363 comprise D1, and a central segment from Ala 145 to Lys 284 makes up domain D2. The last six residues of FlgE31 were invisible in the electron density map. Both domains have an oval shape and are made mostly of β-structures. Domain D2 is a flattened, eight-strand β-barrel but with significant irregularity and extra loops. Domain D1 has a rather complex, unusual fold composed of many different folding motifs: a stack of four horizontal β-hairpins one above another, alternating their orientations with crossing angles of about 120° (Asn 79–Leu 115 and Gly 324–Gln 337, on the left side in Fig. 1); a triangular loop (Thr 116–Pro 135, on the right side in front); a four-stranded (Leu 288–Ile 314 and Asn 357–Ser 363) and a two-stranded (Val 315–Asn 321 and Ser 339–Thr 346) β-sheet (in the upper and lower half, respectively, both on the back side); two consecutive β-turns (Thr 346–Phe 352, behind the triangular loop); and a vertically extended chain (Pro 135–Ala 144, in the centre front of the upper half). This extended chain seems to be a backbone around which the other motifs assemble. A three-dimensional structural similarity search using software DALI[25] resulted in no match for domain D1, confirming its unique fold. The longest dimensions of domain D1 and D2 are about 50 and 45 Å, respectively, and these two domains are connected along their long axes with an angle of about 70°.

As predicted from amino acid sequences and expected from far-ultraviolet circular dichroic spectra, the structure of FlgE31 is very different from that of the F41 fragment of flagellin[21,26], which consists of three domains with domain D1, which consists of three α-helices and a β-hairpin, domain D2, which is formed from many β-hairpins, and domain D3, which is made of a tight β-barrel. It is curious that these two molecules with completely different structures both form the tubular structures with basically the same architecture and helical symmetry.

Partial atomic model of the hook

To build a model of the hook, we then obtained a three-dimensional image reconstruction of a straight hook by using electron cryo-microscopy and image analysis, and docked the crystal structure of FlgE31 in the density map, the details of which will be described elsewhere (T.R.S., D.R.T., J.Z.C., F.A.S., H.M., K.I., K.N., D.J.D, manuscript in preparation). The density map of the hook showed three domains: the outermost domain on the surface of the hook at a radius of 7.5 nm, the middle domain that lies between radii of 5 and 6 nm, and inner core domain that forms a tube with a wall about 1 nm thick and a 3-nm axial lumen. The inner core domain, which is rod-shaped, about 1 nm in diameter and about 2.5 nm long, is most likely to be an α-helical coiled coil made of both terminal chains of FlgE, just like the one seen in the atomic model of flagellin in the filament[26]. The two-domain structure of FlgE31 was therefore docked into the middle and outer domains of the hook density map.

The initial docking was performed manually by fitting each domain separately, with domain D2 into the outer density feature and D1 into the middle one, on the basis of the reasonable assumption that the terminal chains of FlgE are located in the inner core of the hook in a similar way to those of flagellin in the filament[26]. The two domains were then connected, and the hook model was refined with a real-space structure refinement program[27]. The atomic model of the hook in a Cα backbone ribbon diagram is superimposed on the density map in Fig. 2a, b, showing that the model fits nicely in the density. The correctness of this hook model

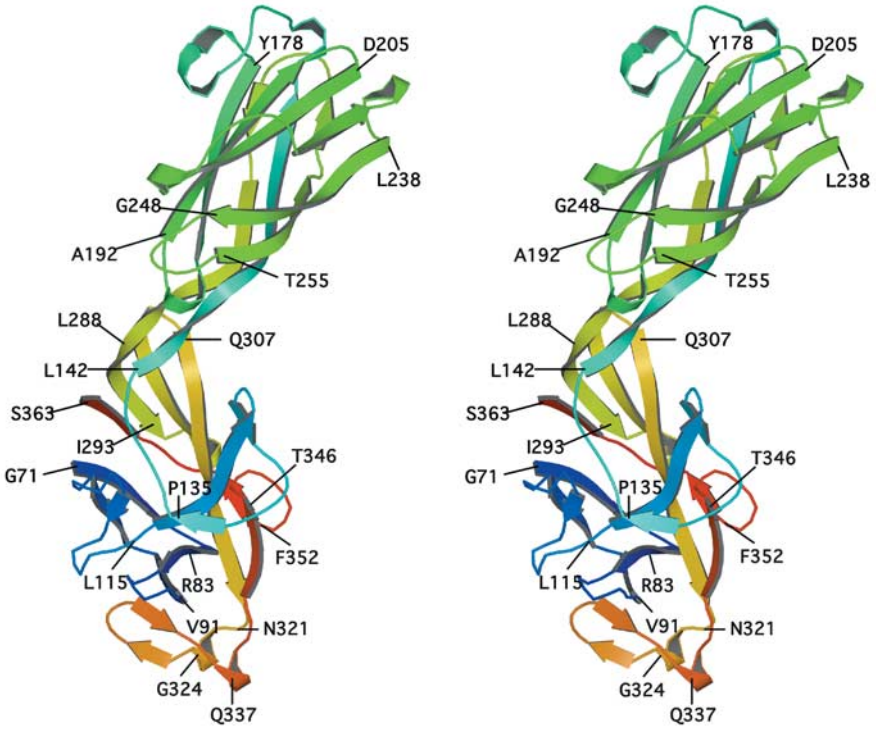

Figure 1 Stereo view of the Cα backbone trace of FlgE31. The chain is colour-coded from blue to red, going through the rainbow colours, from the N terminus to the C terminus. The model is oriented with domain D1 at the bottom and D2 at the top. Domain D1 shows a stack of four β-hairpins on the left and a triangular loop on the front right. All figures were prepared with MOLSCRIPT[45] and RASTER3D[46].

©2004 Nature Publishing Group

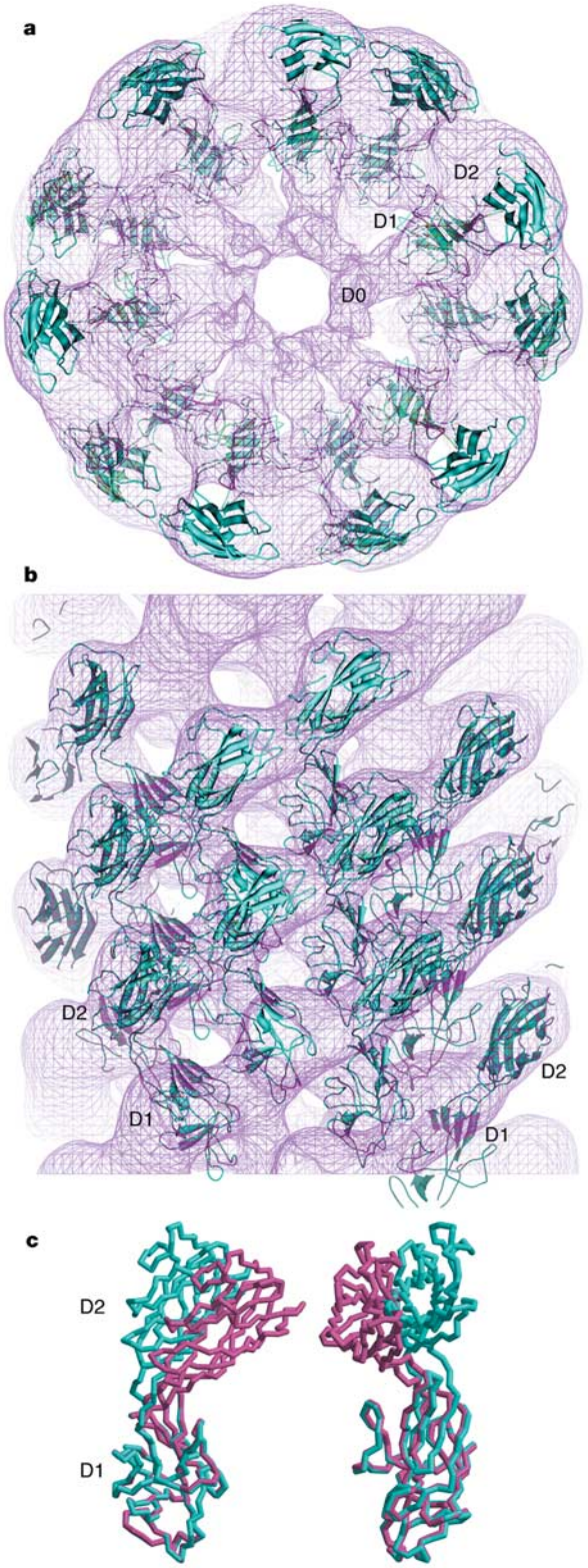

Figure 2 Docking of the atomic model of FlgE31 into the outer two domains of the hook. **a**, End-on view. **b**, Side view. In the side view, slightly more than half of the hook density on the back is trimmed off for clarity. **c**, Change in the relative domain arrangement involved in the docking and refinement. Two different views are presented. The models are colour-coded as follows: purple, crystal structure; cyan, refined model.

will be discussed in more detail elsewhere (T.R.S., D.R.T., J.Z.C., F.A.S., H.M., K.I., K.N., D.J.D, manuscript in preparation). The relative orientations of the major axes of domains D1 and D2 had to be changed for the docking and refinement as shown in Fig. 2c. The change in angle between the major axes is small but the two domains had to be twisted with respect to each other by about 10°, indicating that the hinge at the D1–D2 connection is relatively flexible. This flexibility in the subunit conformation seems to have an important function in the mechanical property of the hook, as discussed below.

Interactions between subunits

It has been indicated even in density maps of relatively low resolution[11,19] that the packing interactions of D2 domains on the hook surface are strong along the 6-start helix, which is a right-handed helical line tilted about 50° to the hook axis. The atomic model as well as the new image reconstruction at higher resolution now shows extensive contacts between D2 domains along the 6-start helix (Figs 2 and 3). D2 domain contacts are found neither along the 11-start helix, which is a nearly axial line, nor the 5-start helix, which is a left-handed helical line at a tilt angle of about 60° (Fig. 4a).

The intersubunit packing interactions between D1 domains on the inside of the straight hook are not very extensive in any of the three helical directions described above, but show more or less equally weak contacts between side chains (Fig. 4a). The top and bottom portions of the stacked β-hairpins have interactions along the 5-start and 6-start, respectively, with the C-terminal chains on the lower and upper sides of domain D1, respectively. The top to bottom interaction along the 11-start is made between the C-terminal chains. The residues involved in these interactions are summarized in Supplementary Table 1.

Along the 11-start helices there are intimate intersubunit interactions between domain D2 of the lower subunit and domain D1 of the upper subunit through the triangular loop of domain D1 (Fig. 4b), where three side-chain contacts are observed (Supplementary Table 1). This is in contrast to the 11-start intersubunit interactions of the flagellar filament. The 11-start direction defines the protofilaments of the flagellar filament, which are the cooperative units that switch between the L and R states to produce the superhelical form of the filament. In the flagellar protofilament, the D1–D1 interactions are much tighter, involving intermolecular β-structure, and its rigidity, which resists axial extension or compression, is important in maintaining the two distinct intersubunit repeat distances of the L and R conformations rather strictly at 52.7 and 51.9 Å, respectively. The presence of both L and R protofilaments in the filament gives rise to its superhelical form; the rigidity of the form is essential to its function as a helical propeller. In contrast, the axial D1–D1 interaction in the hook is only a weak contact involving a few side chains, and its 11-start protofilament structure is mainly held by the D1–D2 interactions with these two domains arranged radially. This is important for its role as a universal joint mechanism as described below.

All the interactions found in the hook model made of domains D1 and D2 are either polar–polar or polar–charge interactions, explaining why FlgE31 cannot polymerize into a stable hook-like fibre structure in aqueous solution. Close interactions between terminal chains in domain D0 in the inner core of the hook are responsible for the stable hook structure formation in a similar way to those of the inner core of the filament[26].

Model of a curved hook

The wild-type hook is highly curved as observed by electron microscopy[4]. Hook protofilaments on the inside of the curve must therefore have shorter repeat distances than those on the outside of the curve, and the difference is much greater than that of the flagellar protofilaments[28]. Although acting as a universal joint, the curvature and curve–linear axis of the hook seem stationary

©2004 Nature Publishing Group

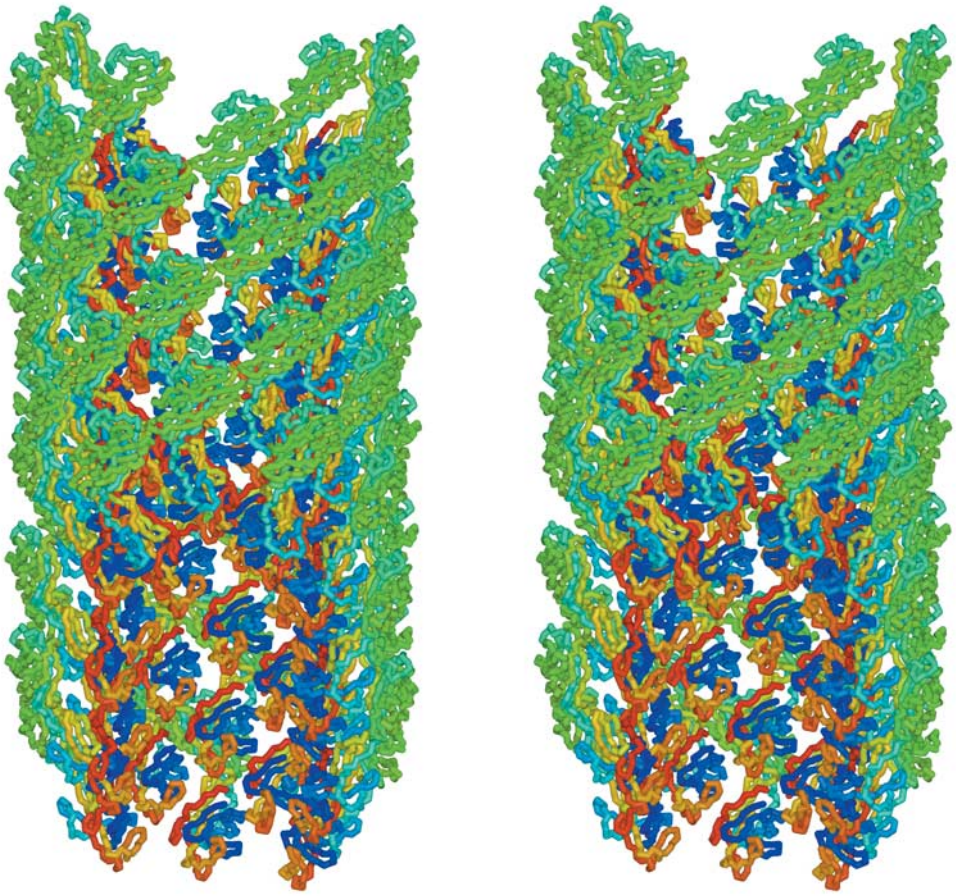

Figure 3 Stereo view of the atomic model of the D1–D2 part of the straight hook. The Cα backbone of each subunit is colour-coded as in Fig. 1. Three of the 11-stranded protofilaments are removed in the front part for the bottom half and in the back for the top half, for clearer views of domain interactions.

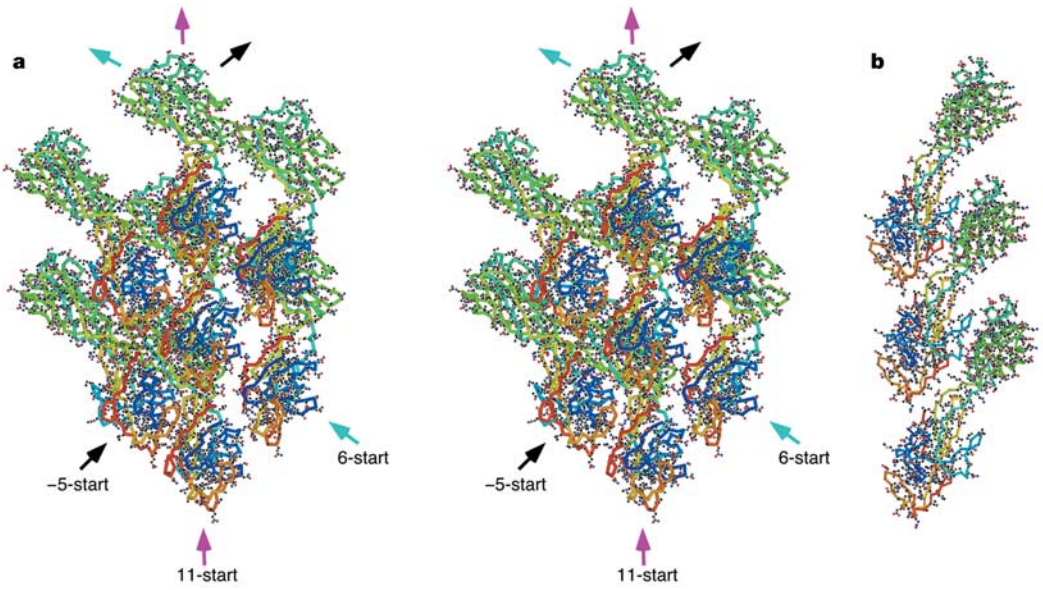

Figure 4 Magnified views of intermolecular interactions along various helical lines of the straight hook. **a**, Seven subunits viewed from the inside (stereo view). **b**, Three subunits along the protofilament (11-start). Atomic models are represented with the Cα backbone in stick form and side chains in ball-and-stick form, and colour-coded as in Fig. 1. Arrows in three different colours in **a** indicate the directions of three representative helical lines: the bottom three for D1 domains and the top three for D2 domains.

©2004 Nature Publishing Group

within the plane containing the axes of the motor and filament; yet, as it rotates, the inside of the bend is successively occupied by different protofilaments. Thus during this kind of rolling rotation, which is like the rotation of smoke in a smoke ring, hook protofilaments must have continuously varying repeat distances and must be going through dynamic conformational changes: an axial extension and a compression with every revolution (Supplementary Videos 1 and 2), occurring about 300 times a second[29,30]. To see the amounts of axial extension and compression and what types of structural change would be responsible for them, we built a preliminary model of a curved hook based on the atomic model of the straight hook. We continuously deformed the helical lattice of the straight hook so that the hook axis conforms a right-handed helical line having a pitch of 950 Å and a diameter of 350 Å as observed previously[18].

The model of the curved hook is shown in Fig. 5a, with a schematic diagram of the basal body at its base. The axial distances between FlgE subunits are made shorter on the inner side and longer on the outer side than those of the straight hook. A short segment of the curved hook is magnified and two 11-start helical arrays, one on the inside and the other on the outside, are shown in Fig. 5b. The near-axial repeat distances between D2 domains on the inside and outside of the curved hook are 35 and 59 Å respectively, whereas those between D1 domains are 39 and 54 Å. In the straight hook these distances are all 46 Å (refs 11, 19); thus, the interdomain distances along the protofilament have to be compressed or extended by about 6–8 Å for the D1 array and by 11–13 Å for the D2 array. The predicted changes in the domain packing are shown magnified in Fig. 5c, d. This is in contrast to the difference in the repeat distance of only 0.8 Å in the protofilament of the filament as mentioned above[31]. How could this large conformational change of the hook protofilament be possible?

The main axial intermolecular interactions that hold the protofilament structure are between domain D1 of the upper subunit and D2 of the lower subunit through the triangular loop of domain D1, which looks like the ampersand character '&' (Figs 4b and 5b). If domains D1 and D2 do not change conformation during rotation of the hook, the only plausible mechanisms for this rather large change in the protofilament repeat distance are either a large conformational change of the triangular loop, which is relatively isolated and independent from the hydrophobic core of domain D1, or a large slip at the interface between the triangular loop and the inner face of domain D2.

We therefore performed a molecular dynamic simulation of extension and compression of the protofilament in a similar way to the simulation that we performed for the flagellar protofilament[21]. We used the atomic model of the isolated hook protofilament made of either two or three subunits, but this time not in a vacuum but surrounded by many water molecules because the model had rather large gaps between domains of interacting subunits. The simulation was done by shifting the reference coordinates of domain D2 of the subunit at the top and domain D1 of the subunit at the bottom in opposite directions and applying positional restraints to the main-chain atoms of these domains to compress by 5 Å or extend by 15 Å (Fig. 6). The conformation of the triangular loop shows relatively small changes after axial compression or extension; instead, the bonding interactions between amino acid residues of the triangular loop and the inner face of D2 show multiple steps of changes in bonding partners (Fig. 6b), realizing a large slippage at this D1–D2 interface, just as shown in Fig. 5b. Certain flexibility in the relative domain orientation between D1 and D2, which was indicated in the docking process of the crystal structure of FlgE31 into the hook density map, seems to have a function in the changes in bonding partners. The bending flexibility of the hook, which is essential for its universal joint function and has actually been observed in electron micrographs of the isolated filament–hook–basal-body complex[4], is probably due to this stepwise axial sliding along with flexibility in relative domain orientation.

Polymorphic supercoiling of the hook

A well-defined switching of the protofilament repeat by 0.8 Å and a

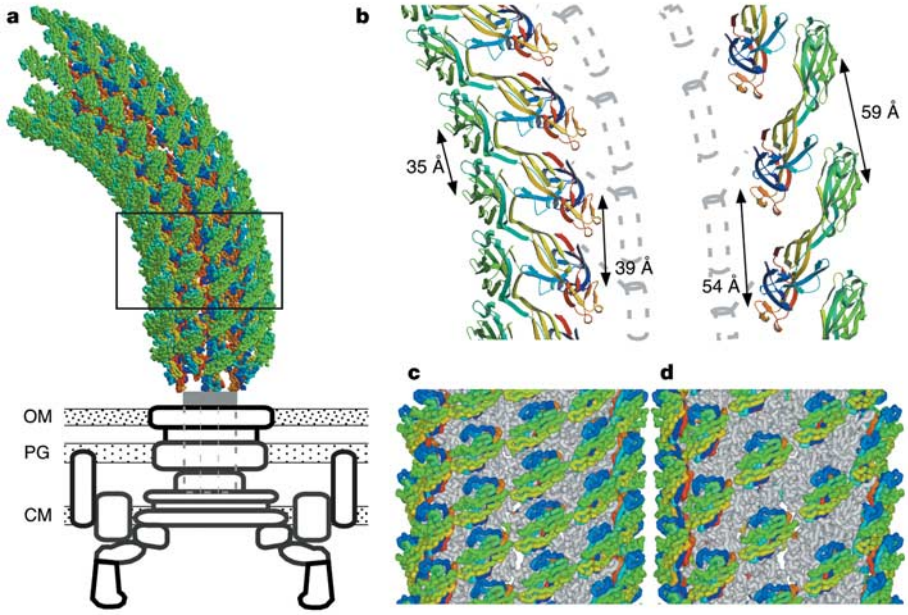

Figure 5 Atomic model of the supercoiled hook. **a**, Atomic model of the coiled hook with a schematic diagram of the basal body spanning the outer membrane (OM) and the cytoplasmic membrane (CM) as well as the peptidoglycan layer (PG). This coiled hook model is part of a supercoiled polyhook with a helical pitch of 950 Å and a diameter of 350 Å. **b**, Magnified image of the coiled hook with the innermost and outermost protofilaments on the left and right, respectively. The inner core domains formed from both terminal chains and the central channel are represented by dotted grey lines. **c**, **d**, Intermolecular packing arrangements of D2 domains on the inner side (**c**) and on the outer side (**d**) of the coiled hook surface. Only domain D2 is colour-coded as in Fig. 1; domain D1 is coloured light grey.

©2004 Nature Publishing Group

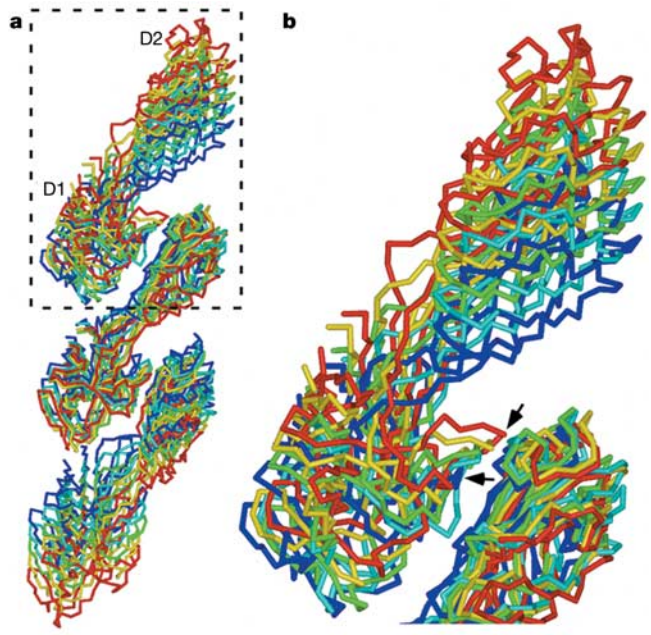

Figure 6 Simulated extension and compression of hook protofilament. Three subunits were used, and domain D2 at the top subunit was moved upwards whereas domain D1 of the bottom subunit was moved downwards. Protofilament models at five different stages at 5 Å intervals are superimposed with different colours: dark blue, light blue, green, yellow and red, from the most compressed to the most extended state. **a**, The whole three subunits. **b**, Magnified view of upper half. D2 domains at the top and D1 domains at the bottom are at equal intervals (2.5 Å) along the vertical axis. It should be noted that the top corner of the triangular loop of domain D1 of the top subunit (indicated by arrows for the most compressed and the most extended, respectively) shows stepwise movements (a jump from dark blue to light blue, very small movements from light blue to green and to yellow, and another jump to red), whereas domain D2 of the middle subunit stays more or less in the same position. This indicates that the triangular loop of domain D1 and the surface of domain D2 can have distinct side-chain bonding partners depending on the state of extension or compression.

relative sliding of neighbouring protofilaments by 2.6 Å are tightly coupled to produce limited sets of twist and curvature for supercoiled flagellar filaments[31]. This is the basis for the polymorphic supercoiling of the filament, in which the cooperatively switching protofilament is important. Kato *et al.*[18] also showed that the polyhook also goes through polymorphic transformations of its supercoiled form in response to changes in the salt concentration, pH and temperature of the solution. Their twist–curvature diagram obtained from the pitch and diameter of helical polyhooks indicated that a two-state model similar to that of the filament might also be valid for the hook, but the inclination angle of the cooperatively switching protofilament to the hook axis in the straight hook is about 50°, much larger than for either of the two types of straight flagellar filament. Assuming a diameter of 200 Å for the hook, which is slightly larger than observed, they suggested that the protofilament must lie along the left-handed 16-start family, but no physical contacts between domains are found along this helical array in the hook model. As shown in the hook model in Figs 2 and 3a, the left-handed 5-start helical array of D1 domains is about 50° to the hook axis; this could therefore be the protofilament for supercoiling. The problem is that the normal polyhook is a right-handed helix, and to make the 5-start helical family have a right-handed inclination the neighbouring domain arrays have to slide to each other over a distance corresponding to about one subunit, which is not a physically plausible mechanism.

An alternative and more plausible mechanism is suggested from the close packing arrangement of D2 domains on the inner side of the curved hook model. If the curvature of the hook is produced by close packing interactions between D2 domains on the inner side while the overall axial repeat of subunits is kept constant by the axial packing interactions of D0 domains in the inner core, which is missing from the present model, a few sets of distinct D2–D2 interactions can define a limited number of virtual protofilament directions to produce distinct supercoils easily, in both left-handed and right-handed forms. The curvature and twist of each supercoil would depend on the direction of the D2–D2 interaction, producing a well-defined distribution of points in the twist–curvature diagram, although it might not necessarily be on a sinusoidal curve as has been observed for the supercoiled filaments. The currently available data do not seem to be sufficient to determine which model is correct. More precise measurements of the pitch and diameter of the polyhooks of various helical forms are necessary to answer this question.

In any case, the structural and functional differences between the hook and the filament are clearly demonstrated here, illustrating the importance and the function of the hook-associated proteins HAP1 and HAP3, which form the hook–filament junction. To join the hook to the filament, HAP1 and HAP3 presumably operate as a structural and mechanical adaptor. Indeed, mutations in HAP3 cause the rotating filament to lose its superhelicity under stress[32]. Although it is not obvious why two proteins are necessary, the structures of HAP1 and HAP3 are expected to have some similarity to those of the hook protein and flagellin, respectively. These two structures have been solved by X-ray crystallography and will be described elsewhere (K.I., H.M., F.A.S., S.N. and K.N., manuscript in preparation). □

Methods

Preparation and crystallization of FlgE31

The preparation and crystallization of FlgE31 from *Salmonella typhimurium* will be described elsewhere[33]. In brief, with the use of the hanging drop vapour diffusion method, crystals were obtained by equilibrating a protein solution containing 1.5 mg ml^{-1} FlgE31, 6% PEG-2000, 1.5 mM cuprous acetate, 25 mM sodium cacodylate, with a reservoir solution consisting of 12% poly(ethylene glycol) (2000 Da), 3 mM cuprous acetate, 50 mM sodium cacodylate, pH 4.5. Crystals appeared after 10 days and the biggest crystal grew to about 0.8 mm × 0.2 mm × 0.3 mm.

Data collection and structure analysis

FlgE31 crystals were frozen in liquid propane equilibrated with liquid nitrogen. All the data sets were collected at temperatures of about 100 K. The native data set was collected at beamline ID29 at the European Synchrotron Radiation Facility, Grenoble. The space group of the crystal is $P2_12_12$, with cell dimensions $a = 128.7$ Å, $b = 49.0$ Å, $c = 96.9$ Å. The solvent content is 48% and the crystal contains two molecules per asymmetric unit. A set of multi-wavelength anomalous diffraction (MAD) data, which produced a high-quality electron density map at 2.3 Å resolution, were collected at beamline BL41XU at the 8-GeV Super Photon ring (SPring-8) in Harima. The data were reduced by DENZO and SCALEPACK[34], or MOSFLM[35] and SCALA[36]. The phases at 2.3 Å were obtained from the set of MAD data and SOLVE[37]. The phases were extended by density modification to 1.8 Å with RESOLVE[37,38]. Partial tracing of the chain was performed with ARP/WARP[39] and completed with O[40]. The model was refined at 1.8 Å resolution including 763 water molecules (Supplementary Table 2) with REFMAC5 (refs 36, 41). In the final model of FlgE31, the six last residues in the C-terminal chain could not be traced because of the poor quality of the density map at this end.

Electron cryomicroscopy and helical image analysis

Polyhooks were isolated as described previously[42]. Grids were prepared for electron cryomicroscopy with the use of protocols for flagellar filaments[43] except that grids were prepared at 4 °C, which straightened about 50% of the normally curly hooks. Electron microscopy was performed at 200 keV with a field emission gun at about × 65,000 magnification and a range of underfocus from 1.3 to 2.7 μm and a dose of 10 electrons Å^{-2}. We cut digitized images (pixel size 3.2 Å) of frozen-hydrated polyhooks into 420 total polyhook segments of about 800 hook subunits. The segments that failed to reveal at least three layer-lines in their Fourier transforms were subsequently rejected. Layer-line data sets from the remaining 354 images were aligned and merged by using cross-correlation methods. Further details of the helical image analysis, three-dimensional image reconstruction, and docking of the atomic model into the density will be fully described elsewhere (T.R.S., D.R.T., J.Z.C., F.A.S., H.M., K.I., K.N., D.J.D, manuscript in preparation; details are available from the authors on request). Fourier data out to 9 Å resolution have been included in the three-dimensional image reconstruction although the true resolution may not be as good as that.

©2004 Nature Publishing Group

Simulated extension and compression of the protofilament

Molecular dynamics simulation was performed by using the module SANDER in the molecular simulation program package AMBER7 (ref. 44) with the parm99 force field. As the isolated hook protofilament model, the atomic model consisting of two or three FlgE31 subunits was initially placed in a rectangular box. The gaps were filled with water molecules and counterions. To allow the large extension of inter-subunit distances, the margin from the subunit to the boundary was initially set to be at least 25 Å along the *z*-axis. The initial box size, the number of water molecules, sodium ions and total atoms were 89.1 Å × 81.3 Å × 191.6 Å, 36,567, 18 and 118,149 in the two-subunit simulation and 92.6 Å × 89.2 Å × 237.9 Å, 52,165, 27 and 169,167 in the three-subunit simulation, respectively. Periodic boundary conditions were used and non-bonded interactions were calculated by the particle-mesh Ewald method. After equilibration in an isothermal–isobaric ensemble at 300 K and 1 atm, the reference coordinates of domain D2 of the subunit at the top and domain D1 of the subunit at the bottom were shifted in opposite directions along the protofilament axis, and positional restraints were applied to the main-chain atoms so as to displace these domains to the position of the reference coordinates. The stepwise shift of the reference coordinates was made by 1 Å, up to 15 Å in extension and up to 5 Å in compression. In each step, 10-ps molecular dynamics simulation was performed and the final coordinate was used for the analysis.

Received 1 July; accepted 8 September 2004; doi:10.1038/nature02997.

1. Macnab, R. M. How bacteria assemble flagella. *Annu. Rev. Microbiol.* **57,** 77–100 (2003).
2. Berg, H. C. The rotary motor of bacterial flagella. *Annu. Rev. Biochem.* **72,** 19–54 (2003).
3. Kojima, S. & Blair, D. The bacterial flagellar motor: structure and function of a complex molecular machine. *Int. Rev. Cytol.* **233,** 93–134 (2004).
4. DePamphilis, M. L. & Adler, J. Purification of intact flagella from *Escherichia coli* and *Bacillus subtilis*. *J. Bacteriol.* **105,** 376–383 (1971).
5. DePamphilis, M. L. & Adler, J. Fine structure and isolation of the hook–basal body complex of flagella from *Escherichia coli* and *Bacillus subtilis*. *J. Bacteriol.* **105,** 384–395 (1971).
6. Berg, H. C. & Anderson, R. A. Bacteria swim by rotating their flagellar filaments. *Nature* **245,** 380–382 (1973).
7. Silverman, M. & Simon, M. Flagellar rotation and the mechanism of bacterial motility. *Nature* **249,** 73–74 (1974).
8. Namba, K. & Vonderviszt, F. Molecular architecture of bacterial flagellum. *Q. Rev. Biophys.* **30,** 1–65 (1997).
9. Macnab, R. M. & Ornston, M. K. Normal-to-curly flagellar transitions and their role in bacterial tumbling. Stabilization of an alternative quaternary structure by mechanical force. *J. Mol. Biol.* **112,** 1–30 (1977).
10. Turner, L., Ryu, W. S. & Berg, H. C. Real-time imaging of fluorescent flagellar filaments. *J. Bacteriol.* **182,** 2793–2801 (2000).
11. Wagenknecht, T., DeRosier, D. J., Aizawa, S.-I. & Macnab, R. M. Flagellar hook structures of *Caulobacter* and *Salmonella* and their relationship to filament structure. *J. Mol. Biol.* **162,** 69–87 (1982).
12. Kagawa, H., Aizawa, S. I. & Asakura, S. Transformations in isolated polyhooks. *J. Mol. Biol.* **129,** 333–336 (1979).
13. Williams, A. W. *et al.* Mutation in fliK and flhB affecting flagellar hook and filament assembly in *Salmonella typhimurium*. *J. Bacteriol.* **178,** 2960–2970 (1996).
14. Hirano, T., Yamaguchi, S., Oosawa, K. & Aizawa, S.-I. Roles of FliK and FlhB in the determination of flagellar hook length in *Salmonella typhimurium*. *J. Bacteriol.* **176,** 5439–5449 (1994).
15. Wagenknecht, T., DeRosier, D. J., Shapiro, L. & Weissborn, A. Three-dimensional reconstruction of the flagellar hook from *Caulobacter crescentus*. *J. Mol. Biol.* **151,** 439–465 (1981).
16. Kutsukake, K., Suzuki, T., Yamaguchi, S. & Iino, T. Role of gene flaFV on flagellar hook formation in *Salmonella typhimurium*. *J. Bacteriol.* **140,** 267–275 (1979).
17. Aizawa, S. & Maeda, Y. A new method for determination of parity in optical diffraction patterns from the structures with helical symmetry. *J. Mol. Biol.* **137,** 437–442 (1980).
18. Kato, S., Okamoto, M. & Asakura, S. Polymorphic transition of the flagellar polyhook from *Escherichia coli* and *Salmonella typhimurium*. *J. Mol. Biol.* **173,** 463–476 (1984).
19. Morgan, D. G., Macnab, R. M., Francis, N. R. & DeRosier, D. J. Domain organization of the subunit of the *Salmonella typhimurium* flagellar hook. *J. Mol. Biol.* **229,** 79–84 (1993).
20. Homma, M., DeRosier, D. J. & Macnab, R. M. Flagellar hook and hook-associated proteins of *Salmonella typhimurium* and their relationship to other axial components of the flagellum. *J. Mol. Biol.* **213,** 819–832 (1990).
21. Samatey, F. A. *et al.* Structure of the bacterial flagellar protofilament and implications for a switch for supercoiling. *Nature* **410,** 331–337 (2001).
22. Samatey, F. A., Imada, K., Vonderviszt, F., Shirakihara, Y. & Namba, K. Crystallization of the F41 fragment of flagellin and data collection from extremely thin crystals. *J. Struct. Biol.* **132,** 106–111 (2000).
23. Vonderviszt, F., Ishima, R., Akasaka, K. & Aizawa, S. Terminal disorder: a common structural feature of the axial proteins of bacterial flagellum? *J. Mol. Biol.* **226,** 575–579 (1992).
24. Vonderviszt, F., Zavodszky, P., Ishimura, M., Uedaira, H. & Namba, K. Structural organization and assembly of flagellar hook protein from *Salmonella typhimurium*. *J. Mol. Biol.* **251,** 520–532 (1995).
25. Holm, L. & Sander, C. Protein structure comparison by alignment of distance matrices. *J. Mol. Biol.* **233,** 123–138 (1993).
26. Yonekura, K., Maki-Yonekura, S. & Namba, K. Complete atomic model of the bacterial flagellar filament by electron cryomicroscopy. *Nature* **424,** 643–650 (2003).
27. Chen, J. Z., Fürst, J., Chapman, M. S. & Grigorieff, N. Low resolution structure refinement in electron microscopy. *J. Struct. Biol.* **144,** 144–151 (2003).
28. Hasegawa, K., Yamashita, I. & Namba, K. Quasi- and nonequivalence in the structure of bacterial flagellar filament. *Biophys. J.* **74,** 569–575 (1998).
29. Lowe, G., Meister, M. & Berg, H. C. Rapid rotation of flagellar bundles in swimming bacteria. *Nature* **325,** 637–640 (1987).
30. Kudo, S., Magariyama, Y. & Aizawa, S. Abrupt changes in flagellar rotation observed by laser dark-field microscopy. *Nature* **346,** 677–680 (1990).
31. Yamashita, I. *et al.* Structure and switching of bacterial flagellar filaments studied by X-ray fiber diffraction. *Nature Struct. Biol.* **5,** 125–132 (1998).
32. Fahrner, K. A., Block, S. M., Krishnaswamy, S., Parkinson, J. S. & Berg, H. C. A mutant hook-associated protein (HAP3) facilitates torsionally induced transformations of the flagellar filament of *Escherichia coli*. *J. Mol. Biol.* **238,** 173–186 (1994).
33. Samatey, F. A., Matsunami, H., Imada, K., Nagashima, S. & Namba, K. Crystallization of a core fragment of the hook protein FlgE. *Acta Crystallogr. D* (in the press).
34. Otwinowski, Z. & Minor, W. *Processing of X-ray Diffraction Data Collected in Oscillation Mode* (Academic, New York, 1997).
35. Powell, H. R. The Rossmann Fourier autoindexing algorithm in MOSFLM. *Acta Crystallogr. D* **55,** 1690–1695 (1999).
36. Collaborative Computational Project No. 4, The CCP4 suite: Programs for protein crystallography. *Acta Crystallogr. D* **50,** 760–763 (1994).
37. Terwilliger, T. C. & Berendzen, J. Automated structure solution for MIR and MAD. *Acta Crystallogr. D* **55,** 849–861 (1999).
38. Terwilliger, T. C. Maximum-likelihood density modification. *Acta Crystallogr. D* **56,** 965–972 (2000).
39. Perrakis, A., Morris, R. & Lamzin, V. S. Automated protein model building combined with iterative structure refinement. *Nature Struct. Biol.* **6,** 458–463 (1999).
40. Jones, T. A., Zhou, J. Y., Cowan, S. W. & Kjeldgaard, M. Improved methods for building protein models in electron density maps and the location of errors in these models. *Acta Crystallogr. A* **47,** 110–119 (1991).
41. Murshudov, G. N., Vagin, A. A. & Dodson, E. J. Refinement of macromolecular structures by the maximum-likelihood method. *Acta Crystallogr. D* **53,** 240–255 (1997).
42. Francis, N. R., Sosinsky, G. E., Thomas, D. & DeRosier, D. J. Isolation, characterization and structure of bacterial flagellar motors containing the switch complex. *J. Mol. Biol.* **235,** 1261–1270 (1994).
43. Morgan, D. G., Owen, C., Melanson, L. A. & DeRosier, D. J. Structure of bacterial flagellar filaments at 11 Å resolution: packing of the alpha-helices. *J. Mol. Biol.* **249,** 88–110 (1995).
44. Case, D. A., *et al.* AMBER7. (Univ. California, San Francisco, California, 2002).
45. Kraulis, P. J. MOLSCRIPT: a program to produce both detailed and schematic plots of protein structures. *J. Appl. Crystallogr.* **24,** 946–950 (1991).
46. Merritt, E. A. & Bacon, D. J. Raster3D: Photorealistic molecular graphics. *Methods Enzymol.* **277,** 505–524 (1997).

Supplementary Information accompanies the paper on **www.nature.com/nature**.

Acknowledgements We thank R. M. Macnab, who passed away suddenly in September 2003, for his invaluable discussion on the structure and function of the flagellar hook; the staff members of beamline ID29 at the European Synchrotron Radiation Facility (ESRF) in Grenoble and beamline BL41XU at the 8 GeV Super Photon ring (SPring-8) in Harima for their help for the data collection; and F. Oosawa and S. Asakura for continuous support and encouragement.

Competing interests statement The authors declare that they have no competing financial interests.

Correspondence and requests for materials should be addressed to K.N. (keiichi@fbs.osaka-u.ac.jp). Atomic coordinates have been deposited in the Protein Data Bank under accession code 1WLG.

©2004 Nature Publishing Group